Proc. Natl. Acad. Sci. USA
Vol. 96, pp. 10717–10722, September 1999
Cell Biology

Targeted disruption of the β adducin gene (*Add2*) causes red blood cell spherocytosis in mice

DIANA M. GILLIGAN*†, LARISSA LOZOVATSKY*, BABETTE GWYNN‡, CARLO BRUGNARA§, NARLA MOHANDAS¶, AND LUANNE L. PETERS‡

*Department of Internal Medicine (Hematology), Yale University School of Medicine, New Haven, CT 06510; ‡The Jackson Laboratory, Bar Harbor, ME 04609; §Department of Laboratory Medicine, Children's Hospital, Boston, MA 02115; and ¶Lawrence Berkeley National Laboratory, University of California, Berkeley, CA 94720

Communicated by Edward A. Adelberg, Yale University, New Haven, CT, July 8, 1999 (received for review May 25, 1999)

ABSTRACT **Adducins are a family of cytoskeleton proteins encoded by three genes (α, β, γ). In a comprehensive assay of gene expression, we show the ubiquitous expression of α- and γ-adducins in contrast to the restricted expression of β-adducin. β-adducin is expressed at high levels in brain and hematopoietic tissues (bone marrow in humans, spleen in mice). To elucidate adducin's role *in vivo*, we created β-adducin null mice by gene targeting, deleting exons 9–13. A 55-kDa chimeric polypeptide is produced from the first eight exons of β-adducin and part of the neo cassette in spleen but is not detected in peripheral RBCs or brain. β-adducin null RBCs are osmotically fragile, spherocytic, and dehydrated compared with the wild type, resembling RBCs from patients with hereditary spherocytosis. The lack of β-adducin in RBCs leads to decreased membrane incorporation of α-adducin (30% of normal) and unexpectedly promotes a 5-fold increase in γ-adducin incorporation into the RBC membrane skeleton. This study demonstrates adducin's importance to RBC membrane stability *in vivo*.**

Adducin was originally described as a protein kinase C substrate in RBCs (1). Purified human RBC adducin consists of two similar polypeptides, α (M_r of 103,000) and β (M_r of 97,000) (2). *In vitro*, RBC adducin crosslinks actin filaments with spectrin in a Ca^{2+}-calmodulin-dependent manner (3), and bundles (4) and caps (5) actin filaments. Adducin is also a substrate for ρ kinase (6, 7) and protein kinase A (8). The third member of the adducin family, γ-adducin, was discovered as a protein kinase C binding protein in kidney (9). γ-adducin, a doublet of 84,000 and 86,000 M_r, interacts with α-adducin in kidney cell extracts (9). Alternatively spliced mRNAs have been described from all three adducin genes (10, 11). Most encode truncated isoforms compared with the originally described isoforms, and their functions are not yet known. To determine the function of β-adducin *in vivo*, we created a null mutation in mice. β-adducin null RBCs are osmotically fragile and demonstrate properties similar to RBCs from patients with hereditary spherocytosis. This study demonstrates adducin's importance in RBC structure *in vivo*.

MATERIALS AND METHODS

Targeted Disruption of the β-Adducin Gene (*Add2*). The targeting vector was constructed in the pPNT (12) plasmid by using a 3.9-kilobase (kb) *Eco*RI-*Bam*HI fragment as the 5′ homology segment and a 1.9-kb *Eco*RI-*Not*I fragment as the 3′ homology segment (Fig. 3*A*). Transfected 129/Sv-derived J1 embryonic stem cells (12) were cultured and selected in G418 and gancyclovir. Genomic DNA was digested with *Eco*RV and was analyzed by Southern blotting using a flanking *Eco*RV-*Eco*RI fragment as the hybridization probe (Fig. 3*B*). Blastocyst injection and embryo transfer were performed by using standard techniques (13). Male chimeras were mated to C57BL/6J females to generate heterozygotes. Progeny were genotyped by using PCR on tail biopsies.

Red Blood Cell Analysis. Blood counts were determined by using a Technicon H3 analyzer (Bayer Diagnostics, Tarrytown, NY). Smears were stained with Wright-Giemsa (Sigma). Reticulocytes were counted manually after staining with new methylene blue.

Osmotic Gradient Ektacytometry. Fresh RBCs were mixed continuously with a 4% polyvinylpyrrolidone solution of increasing osmolality (60–600 mosM). The deformability index was recorded as a function of osmolality at a constant applied shear stress of 170 dynes/cm^2 by using an ektacytometer (Bayer Diagnostics) (14).

Osmotic Fragility. Osmotic fragility was measured in cells washed three times in mouse isotonic saline (340 mosM) and resuspended at a final hematocrit of ≈5%. Ten microliters was added to two-hundred and ninety microliters of lysis medium in microplates and was incubated at room temperature for 20 min. After gentle centrifugation, supernatant was removed, and percent lysis was calculated from the absorbance at 540 nm. Lysis medium contained either 2 mM Tris·Hepes or 159 mM NaCl and 2 mM Tris·Hepes, or combinations of these two media (range 120–325 mosM, pH 7.5 at 20°C). RBC Na^+ and K^+ content were measured as described (15).

SDS/PAGE and Western Blotting. Whole blood was collected in acid citrate dextrose by retroorbital phlebotomy or cardiac puncture of anesthetized mice. RBCs and platelet-rich plasma were separated by centrifugation at 120 × *g* for 20 min. RBCs and platelets were washed with murine PBS (10 mM NaCl/155 mM KCl/10 mM glucose/1 mM $MgCl_2$/2.5 mM $KHPO_4$, pH 7.4) containing 1–4 mM pefabloc protease inhibitor (Boehringer Mannheim). Washed platelets were dissolved with Laemmli sample buffer and were boiled for 10 min. Hemoglobin-depleted RBC ghosts were prepared as described (2). SDS/PAGE was performed by the method of Fairbanks as modified by Steck (16) or by the method of Laemmli (17).

Tissue samples were dissected from mice after perfusion with PBS, were placed immediately in liquid nitrogen, and were stored at −80°C until use. Samples were homogenized in 0.32 M sucrose in PBS containing 1–4 mM pefabloc. A low speed (2,500 rpm × 5 min) pellet of nuclei and debris was discarded. Samples then were fractionated into 30,000 × *g* pellet and supernatant fractions, consisting of crude membranes and cytoplasm, respectively. Samples were dissolved in Laemmli buffer and were run on 4–15% gradient SDS-

The publication costs of this article were defrayed in part by page charge payment. This article must therefore be hereby marked "*advertisement*" in accordance with 18 U.S.C. §1734 solely to indicate this fact.

PNAS is available online at www.pnas.org.

Abbreviation: kb, kilobase.

†To whom reprint requests should be addressed at: Department of Internal Medicine (Hematology), Yale University School of Medicine, WWW 403, 333 Cedar Street, New Haven, CT 06510. E-mail: Diana.Gilligan@yale.edu.

polyacrylamide gels. Samples on duplicate gels were stained by Coomassie blue or were transferred to nitrocellulose. Blots were blocked in PBS-Triton-BSA [0.15 M NaCl, 0.1 mM EDTA, and 10 mM $NaHPO_4$ (pH 7.4) with 0.2% Triton X-100 and 3% BSA), were incubated with primary antibody in PBS-Triton-BSA overnight at 4°C, were washed, and were incubated with peroxidase-protein A (Bio-Rad) in PBS-Triton-BSA at 22°C for 1 hour. Blots were washed and incubated with chemiluminescence substrate (Amersham Pharmacia) and were exposed to x-ray film (Kodak). Films were scanned by using a Molecular Dynamics Computing Densitometer.

Antibodies. All antibodies were affinity-purified from rabbit serum. α- and β-adducin antibodies, a gift from H. Clive Palfrey (University of Chicago), were raised against full-length human RBC adducin and have been described previously (18). The γ-adducin antibody, a gift from Susan Jaken (University of Vermont), was raised against recombinant peptide comprising amino acids 467–674, the carboxy terminus (9). The NH_2-terminal β-adducin antibody was raised against a mixture of six synthetic peptides (a gift from Vann Bennett, Duke University) corresponding to the following amino acids from human β-1 adducin (19): 126–145, 336–362, 422–445, 446–471, 463–480, 696–721. An antibody to the carboxy terminus of β-1 was made by using a recombinant polypeptide comprising amino acids 538–726 from human β-1 adducin.

Northern Blotting. Total RNA was isolated by using the guanidinium thiocyanate-phenol-chloroform method (20). Northern blotting was performed by standard techniques. Hybridization was carried out at 42°C in formamide and washing at 65°C.

Histology/Electron Microscopy. Mice were anesthetized and perfused with 20 ml of Bouin's fixative. Tissues were placed in fresh fixative overnight and were processed to paraffin. Sections (5 μm) were stained with hematoxylin and eosin for routine examination and with Prussian blue to detect iron. Scanning electron microscopy of fixed, whole red blood cells was performed as described (21).

RESULTS

The Adducins Are Widely Expressed in Mouse and Human Tissues. We examined adducin expression by using a multiple tissue expression array with mRNA from 76 human tissues and cell lines. Human α - and γ- adducin cDNA probes hybridize to every sample in the array, with decreased expression of α-adducin in the tumor cell lines in column 10 (Fig. 1). β-adducin cDNA probes were designed to detect sequences encoding the alternative carboxy termini designated β-1 and β-2 (10). The β-1 probe hybridizes to all neuronal tissues (Fig. 1, columns 1–3) with highest expression in the cerebellum. The β-1 probe also shows high expression in bone marrow (Fig. 1, 7G), fetal brain (11A), and fetal liver (11D) (the site of fetal hematopoiesis). A weak signal is detected in testis (Fig. 1, 8F), fetal spleen (11E), and the K562 cell line (10C). Similarly, the β-2 probe hybridizes to all neuronal and hematopoietic tissues, although the signal is weaker than β-1 (film exposed 7× longer). Surprisingly, the β-2 probe shows expression in lung (Fig. 1, both adult 8A and fetal 11G) whereas β-1 is not expressed in lung.

α- and γ-adducin expression also occur in all mouse tissues examined (Fig. 2). Expression of β-adducin in the mouse is similar to human expression with high levels in brain and spleen (a site of hematopoiesis in the mouse). In brain, the β-1 probe detects a major band at 9–10 kb and minor bands at 6 and 4 kb. In spleen, the β-1 probe detects a major band at 4

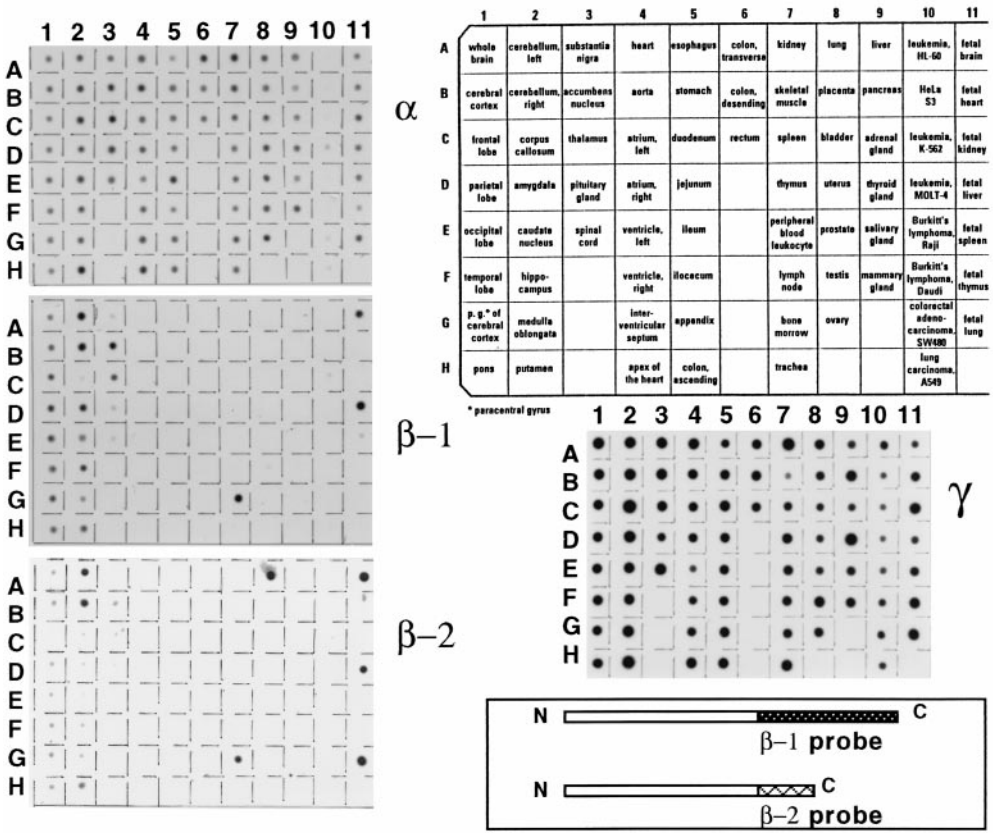

FIG. 1. A multiple-tissue expression array (CLONTECH) of polyA RNA from 76 human tissues and cell lines probed with human cDNAs for α-, β-1, β-2, and γ-adducins. α- and γ-adducins show expression in all samples whereas β-1 and β-2 show restricted expression, mainly in brain and hematopoietic tissues. Probes for β-1 and β-2 were generated by PCR to encompass their distinct carboxy termini and 3′UTRs (β-1, exons 14–17; β2, exon 13b). Subcloned PCR products were labeled by random priming with ^{32}P-dCTP.

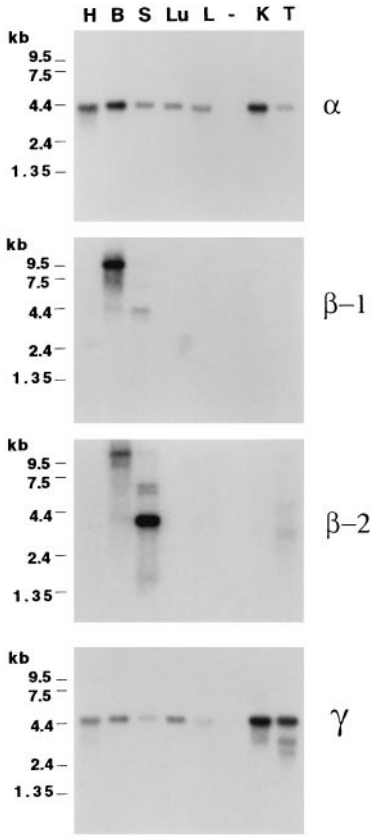

FIG. 2. A multiple-tissue expression Northern blot (CLONTECH) of polyA RNA from seven mouse tissues probed with mouse cDNAs for α, β-1, β-2, and γ-adducins. H, heart; B, brain; S, spleen; Lu, lung; L, liver; K, kidney; T, testis (- is a blank lane). α- and γ-adducin show expression in all lanes whereas β-1 and β-2 show restricted expression, mainly in brain and spleen.

kb and faint bands at 9 and 6 kb. The β-2 probe detects a 9- to 10-kb band in brain, a major 3.8-kb band in spleen, and a minor doublet at 6 kb in spleen.

Targeting of β-Adducin in Mice. To dissect the role of the various adducins *in vivo*, we targeted the β-adducin gene (*Add2*) in mice. Fig. 3*A* shows the β-adducin targeting vector; successful recombination deletes exons 9–13. As one or more of these exons is found in all β-adducin cDNAs described to

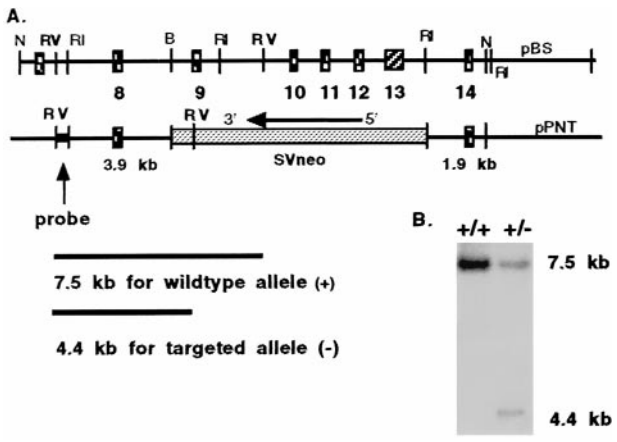

FIG. 3. (*A*) Strategy for targeted deletion of exons 9–13 from *Add2*, the gene encoding β-adducin. (*B*) Southern blot of *Eco*RV-restricted DNA from embryonic stem cell clones electroporated with the vector from *A* and selected for G418 resistance. The probe is indicated in *A* and detects the targeted allele in the clone on the right.

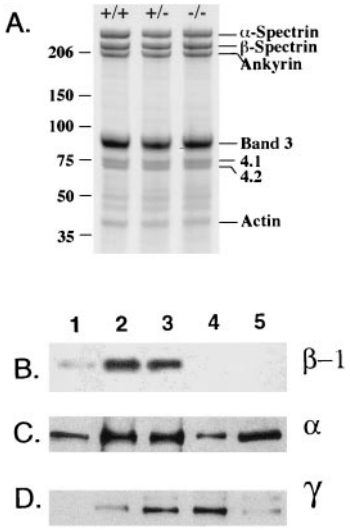

FIG. 4. (*A*) Coomassie blue-stained Steck gel shows no difference in −/− RBC ghosts. (*B–D*) Western blotting of RBC ghosts and platelets. Lanes: 1, human RBC ghosts; 2, +/+ RBC ghosts; 3, +/− RBC ghosts; 4, −/− RBC ghosts; 5, +/+ platelets. Antibodies used for detection are indicated to the right.

date, all isoforms should be disrupted on homologous recombination.

α-Adducin Is Decreased and γ-Adducin Increased in β-Adducin Null RBCs. Homozygous knockout mice are born at the expected Mendelian frequency. Wild-type (+/+), heterozygous (+/−), and homozygous knockout (−/−) mice are indistinguishable at birth. No differences between +/+, +/−, and −/− RBC ghosts are detected by Coomassie blue staining (Fig. 4*A*). Western blotting demonstrates the absence of β-adducin in −/− RBC ghosts (Fig. 4*B*, lane 4). +/− RBC ghosts have reduced β-adducin, 72% of +/+ (Fig. 4*B*, lane 3). As in human platelets, β-adducin is not detected in normal mouse platelets (Fig. 4*B*, lane 5).

In −/− RBC ghosts, α-adducin is reduced to 30% of +/+ levels (Fig. 4*C*, lane 4). In +/− RBC ghosts (Fig. 4*C*, lane 3), α-adducin is normal. An antibody specific for γ-adducin shows a doublet in platelets (Fig. 4*D*, lane 5) and, surprisingly, also detects prominent bands in mouse RBC ghosts but none in human RBC ghosts (Fig. 4*D*, lane 1). The lower band of the doublet is more prominent than the upper band in RBCs compared with platelets. The level of expression of this lower γ-adducin isoform is greatly increased in −/− RBC ghosts (539%) and also in +/− RBC ghosts (377%) compared with +/+.

β-Adducin Null Mice Are Anemic. β-adducin null mice show a phenotype of compensated hemolysis (Table 1). Hematocrits are significantly decreased, and reticulocyte percentages significantly increased. The latter indicates a compensatory acceleration of RBC production in response to chronic hemo-

Table 1. Hematological values in β-adducin knockout mice

	+/+, $n = 11$	−/−, $n = 13$
RBC, $\times 10^{12}$/liter	10.2 ± 0.2	10.7 ± 0.1
HBG, g/dl	16.5 ± 0.3	16.3 ± 0.2
HCT, %	51.4 ± 0.6	47.8 ± 0.5*
MCV, fl	50.6 ± 0.6	44.8 ± 0.5*
MCH, pg	16.2 ± 0.1	15.2 ± 0.1*
MCHC, g/dl	31.9 ± 0.3	34.2 ± 0.4*
Reticulocyte, %	2.8 ± 0.3	4.3 ± 0.4*

All values $x \pm$ SEM. HBG, hemoglobin; HCT, hematocrit; MCV, mean corpuscular volume; MCH, mean corpuscular hemoglobin; MCHC, mean corpuscular hemoglobin concentration.
*$P < 0.05$.

lysis. The decrease in mean corpuscular volume and increase in mean corpuscular hemoglobin concentration are consistent with a loss of membrane surface and dehydration, as seen in cases of hereditary spherocytosis in humans.

β-adducin null RBCs are smaller and show a variety of shapes, including spherocytes, spherostomatocytes, and rounded elliptocytes (Fig. 5 *A* and *B*). Prussian blue staining of the spleen demonstrates increased iron in the −/− spleen (increased erythroblasts as well as phagocytes) compared with the +/+ spleen (Fig. 5*C*). The spleen size also is increased in −/− mice (0.42 vs. 0.26% body weight, $P < 0.05$). Iron deposition also is increased in kidney and liver from −/− mice (data not shown).

Osmotic fragility curves indicate increased osmotic fragility for −/− RBCs (Fig. 6*A*). By osmotic gradient ektacytometry, the maximum value of the deformability index is markedly reduced in −/− RBCs, consistent with loss of membrane surface area (Fig. 6*B*). The Na^+ content of −/− RBCs does not differ from +/+ or +/− RBCs (Fig. 6*C*). Both K^+ content and the total cation content ($Na^+ + K^+$), however, are significantly decreased, consistent with RBC dehydration.

Analysis of Spleen Erythroid Precursors and Nonerythroid Tissues in β-Adducin Null Mice. By Northern blotting (Fig. 7*A*), the expected bands of 9 and 4 kb in brain and 4 kb in spleen are detected in +/+ and +/− mice. Surprisingly, less intense bands of approximately the same size also are seen in the −/− spleen and brain. These bands hybridize to a neoR gene probe (Fig. 7*B*), suggesting that aberrant splicing of the disrupted β-adducin gene has generated mRNA transcripts that include a portion of the *Neo*^{r} gene. Hybridization with a probe derived from exons 9–12 (Fig. 7*C*) does not detect any

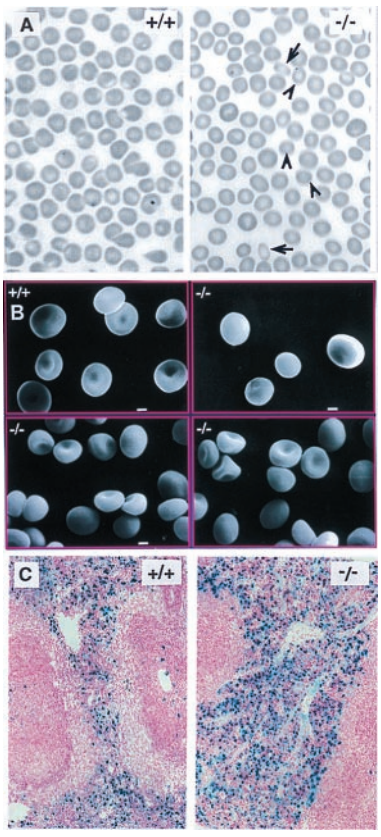

FIG. 5. (*A*) Bright field light microscopy. Arrows indicate rounded elliptocytes; arrowheads indicate microspherocytes. (*B*) Scanning electron microscopy demonstrates that −/− RBCs are smaller and spherocytic compared with +/+ RBCs. (Bar = 1 μm.) (*C*) Increased iron deposition (dark blue color) in spleen from −/− mice compared with +/+ mice.

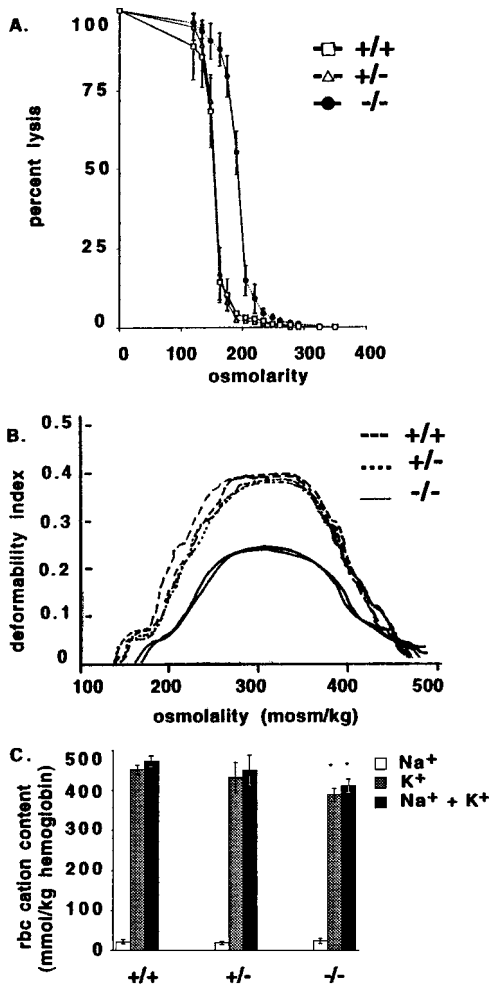

FIG. 6. (*A*) Osmotic fragility curve demonstrates right shift for −/− RBCs. (*B*) Osmotic gradient deformability profiles demonstrate markedly reduced deformability for −/− RBCs; duplicate measurements are shown for each genotype. (*C*) Measurements of cation content show normal Na^+ but decreased K^+ and Na^+ plus K^+ in −/− RBCs.

transcripts in the −/− brain or spleen, confirming that these exons have been deleted.

RT-PCR demonstrates two types of aberrant transcripts in the −/− mice (data not shown). One transcript is a direct splice from exon 8 to exon 14, which does maintain an ORF but does not produce any detectable polypeptide in brain or spleen, based on Western blotting analysis (see below). The second transcript includes a portion of the antisense strand of the neoR gene inserted between exons 8 and 14 of β-adducin. The insertion replaces 743 nt with 491 nt, which is a difference not apparent on Northern blotting (252 nt of 4 and 9 kb) and accounts for the chimeric mRNAs having mobilities very close to the normal mRNAs. This insertion results in coding sequence for an additional 76 amino acids after amino acid 283 before a stop codon is reached. The new amino acids are TYSGSIPSEELVKKAIEGDALRIGSGDTVKHEEAVSPFAAKLFSNITGSQRYVLIAVRHTQPATVDESRKSGHFPP. The calculated molecular weight for this polypeptide is 39,702, although it appears to migrate at a higher M_r (see below), as is true for the normal adducins.

No β-1 adducin is detected in −/− spleen membrane fractions by Western blotting (Fig. 8). However, an additional 55-kDa band is seen on Coomassie blue stained gels in the +/− and −/− spleen supernatant fractions (Fig. 8*A*, arrow). An antibody raised against the β-1 carboxy terminus (amino acids 538–726) encoded by exons 14–17 does not recognize the

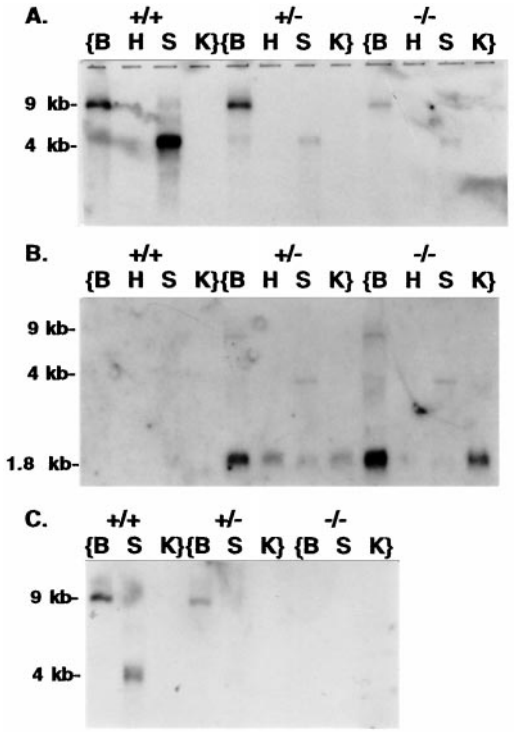

FIG. 7. Northern blotting of total RNA from mouse tissues. B, brain; H, heart; S, spleen; K, kidney. (*A*) Using a full-length β-1 cDNA as probe, 9- and 4-kb mRNAs are detected in brain and spleen. (*B*) Using a probe from the neoR cassette, a 1.8-kb mRNA is seen in all tissues from targeted mice and also hybridizes to the 9- and 4-kb mRNAs from targeted mice. (*C*) Using a probe for the deleted exons 9–12, no mRNA is detected in −/− mice, indicating that the 9- and 4-kb mRNAs are aberrant transcripts inserting antisense neoR sequence in the place of deleted β-adducin exons.

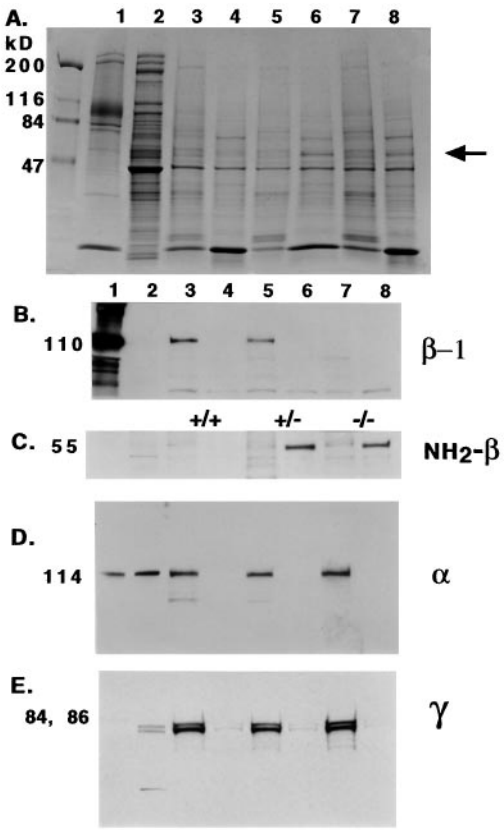

FIG. 8. Western blotting of spleen homogenates. Lanes: 1, human RBC ghosts; 2, human platelets; 3–8, spleen homogenates, separated into 30,000 × *g* pellet (P) and supernatant (S) fractions: 3, +/+ P; 4, +/+ S; 5, +/− P; 6, +/− S; 7, −/− P; 8, −/− S. Gel in *A* is Coomassie blue-stained to demonstrate protein loading. Gels in *B–E* are stained with the antibodies indicated on the right of the panels. The arrow marks the 55-kDa band in lanes 6 and 8 that is immunoreactive to NH_2-β antibody. β-1 is not detected in −/− samples, but α and γ are detected in all pellet samples.

55-kDa band, confirming that it is not the product of the mRNA that splices from exon 8 to exon 14 (data not shown). An antibody raised against synthetic peptides including the amino terminal region of β-adducin does react with this 55-kDa band, suggesting that it is the product of the chimeric mRNA containing β-adducin sequence up to exon 8, followed by sequence and stop codon from the *Neo*^{r} antisense strand (Fig. 8*C*). The localization of this band to the supernatant fraction (cytoplasm), and not to the pellet fraction (membranes and cytoskeleton), suggests that it is not capable of substituting for full length β-1 adducin in the membrane skeleton. Consistent with this observation, the 55-kDa band is not detected in RBC ghosts or intact RBCs by Coomassie blue and Western blotting with the amino-terminal antibody (data not shown).

The loss of β-adducin from spleen does not affect levels of α- or γ-adducin (Fig. 8 *D* and *E*). However, both α- and γ-adducin are much more abundant than β-adducin in the spleen because of their ubiquitous expression including nonerythroid cells. Therefore, changes in their levels of expression in the erythroid compartment, as a result of the absence of β-adducin, may not be detected on preparations of whole spleen.

β-1 adducin is present in both pellet and supernatant fractions from +/+ and +/− brains, but not −/− brains (Fig. 9). Similar to the changes seen in RBC ghosts, α-adducin is decreased and γ-adducin is increased in −/− brains. The presence of adducin in supernatant fractions in brain suggests that some adducin may be soluble and not associated tightly with the membrane skeleton in brain.

At the light microscope level of resolution, there is no detectable difference in the morphology of brains from +/+ and −/− mice (data not shown). There is no obvious difference in behavior of the −/− mice compared with +/+ mice, although more subtle neurological changes are currently being examined.

DISCUSSION

The β-adducin knockout mouse provides the first tool for dissecting the role of adducins in diverse cellular functions *in vivo.* There has not yet been a report of a spontaneous human or mouse mutation in adducin causing hemolytic anemia, so this study is the first demonstration of the importance of adducin in RBC structure.

We demonstrate the expression of two or more adducin genes in all human and mouse tissues examined. It is clear from studies of purified human RBC adducin that the α and β-1 polypeptides are tightly associated in a 1:1 stoichiometry in the membrane skeleton of the mature RBC (22). It is not yet known whether α and γ polypeptides are also tightly associated in a 1:1 stoichiometry in nonerythroid tissues, although α and γ are co-immunoprecipitated from kidney extracts (9). Our results support the existence of an α/γ complex. We observe co-expression of γ with α in all tissues lacking β expression. No tissue shows expression of one adducin gene without a second adducin gene, suggesting that the adducins do not function as monomers. Perhaps the α/γ adducins are a basic component of the cortical skeleton in all cells, with specialized functions

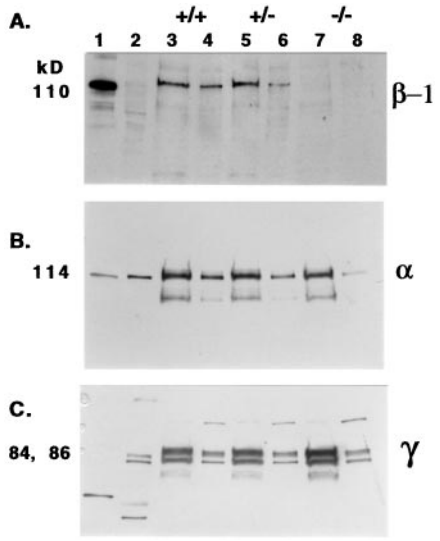

FIG. 9. Western blotting of brain homogenates. Lanes: 1, human RBC ghosts; 2, human platelets; 3–8, brain homogenates, separated into 30,000 × *g* pellet (P) and supernatant (S) fractions: 3, +/+ P; 4, +/+ S; 5, +/− P; 6, +/− S; 7, −/− P; 8, −/− S. β-1 is not detected in −/− samples, but α and γ are detected in all samples.

provided by alternatively spliced isoforms or by the α/β complex.

One reason for deleting β-adducin was to test the hypothesis that α-adducin could function alone in the RBC. The interesting result, however, is that γ- adducin is incorporated into the RBC membrane skeleton instead of β-adducin. Testing the functionality of α-adducin alone will therefore require deletion of both β- and γ-adducins. The expression of γ-adducin in mouse RBCs (even +/+) is a novel species difference because even overloading of human RBCs does not reveal γ-adducin on Western blots. Perhaps the ability to substitute γ-adducin for β-adducin has been lost in humans; mutations in β-adducin in humans might then be lethal. The substitution of γ- for β-adducin and the expression of the truncated 55-kDa amino terminal polypeptide are not sufficient to produce normal RBCs. Although the Western blots demonstrate a 5-fold increase of γ-adducin in −/− RBC ghosts, the absolute amount of γ-adducin in RBC ghosts is not known. Further studies are needed to determine whether the inability of γ-adducin to compensate for lack of β-adducin is a quantitative difference or is a qualitative functional difference between these two isoforms.

Without normal levels of α- and β-adducin, mouse RBCs exhibit many properties typical of hereditary spherocytosis: decreased deformability, increased osmotic fragility, decreased mean corpuscular volume, increased mean corpuscular hemoglobin concentration, and decreased cation content. β-adducin −/− mice also demonstrate increased RBC turnover with increased iron deposition in the spleen, liver, and kidney, larger spleen size, and increased reticulocyte count attributable to compensatory erythropoiesis.

Further studies are in progress to analyze changes in the organization of the RBC membrane skeleton at the electron microscopy level. In particular, the length and number of actin filaments will be quantitated to determine whether actin filament capping has been altered in β-adducin null mice. Perhaps a decreased number of junctional complexes leads to an overall reduction in the ratio of skeleton to membrane, with subsequent membrane loss and spherocytosis.

After RBCs, the brain is the most abundant site of expression of β-adducin. β-adducin −/− brains appear normal by light microscopy, and no major neurological dysfunction has been identified. As in the case of RBCs, γ-adducin may be compensating for the lack of β-adducin in brain, and studying the role of adducin in brain may require deletion of two adducin genes. Alternatively, the effects of the β-adducin knockout on neurological function may become evident with age, as shown for ankyrin deficient mice (23).

We thank H. Clive Palfrey and Susan Jaken for providing antibodies and Vann Bennett for synthetic peptides. D.M.G. was supported by National Institutes of Health Grant DK02070. L.L.P. was supported by National Institutes of Health Grant HL55321 and The March of Dimes. L.L.P. is an Established Investigator of the American Heart Association. M.N. was supported by National Institutes of Health Grant DK26263, and C.B. was supported by National Institutes of Health Grant HL15157.

1. Palfrey, H. C. & Waseem, A. (1985) *J. Biol. Chem.* **260,** 16021–16029.
2. Gardner, K. & Bennett, V. (1986) *J. Biol. Chem.* **261,** 1339–1348.
3. Gardner, K. & Bennett, V. (1987) *Nature (London)* **328,** 359–362.
4. Mische, S. M., Mooseker, M. S. & Morrow, J. S. (1987) *J. Cell Biol.* **105,** 2837–2845.
5. Kuhlman, P. A., Hughes, C. A., Bennett, V. & Fowler, V. M. (1996) *J. Biol. Chem.* **271,** 7986–7991.
6. Kimura, K., Fukata, Y., Matsuoka, Y., Bennett, V., Matsuura, Y., Okawa, K., Iwamatsu, A. & Kaibuchi, K. (1998) *J. Biol. Chem.* **273,** 5542–5548.
7. Fukata, Y., Oshiro, N., Kinoshita, N., Kawano, Y., Matsuoka, Y., Bennett, V., Matsuura, Y. & Kaibuchi, K. (1999) *J. Cell Biol.* **145,** 347–361.
8. Matsuoka, Y., Hughes, C. A. & Bennett, V. (1996) *J. Biol. Chem.* **271,** 25157–25166.
9. Dong, L., Chapline, C., Mousseau, B., Fowler, L., Ramsay, K., Stevens, J. L. & Jaken, S. (1995) *J. Biol. Chem.* **270,** 25534–25540.
10. Gilligan, D. M., L. Lozovatsky & Silberfein, A. (1997) *Genomics* **43,** 141–148.
11. Lin, B., Nasir, J., McDonald, H., Graham, R., Rommens, J. M., Goldberg, Y. P. & Hayden, M. R. (1995) *Genomics* **25,** 93–99.
12. Tybulewicz, V. L. J., Crawford, C. E., Jackson, P. K., Bronson, R. T & Mulligan, R. C. (1991) *Cell* **65,** 1153–1163.
13. Robertson, E. J. (1987) *Teratocarcinomas and Embryonic Stem Cells: A Practical Approach.* (IRL, Oxford).
14. Clark, M. R., Mohandas, N. & Shohet, S. B. (1983) *Blood* **61,** 899–910.
15. Armsby, C. C., Brugnara, C. & Alper, S. L. (1995) *Am. J. Physiol.* **268,** C894–C902.
16. Steck, T. L. (1974) *J. Cell Biol.* **62,** 1–19.
17. Laemmli, U. K. (1970) *Nature (London)* **227,** 680–685.
18. Waseem, A. & Palfrey, H. C. (1988) *Eur. J. Biochem.* **178,** 563–573.
19. Joshi, R., Gilligan, D. M., Otto, E., McLaughlin, T. & Bennett, V. (1991) *J. Cell Biol.* **115,** 665–675.
20. Chomczynski, P. & Sacchi, N. (1987) *Anal. Biochem.* **162,** 156–159.
21. Peters, L. L., Birkenmeier, C. S. & Barker, J. E. (1992) *Blood* **80,** 2122–2127.
22. Hughes, C. A. & Bennett, V. (1995) *J. Biol. Chem.* **270,** 18990–18996.
23. Peters, L. L. & Barker, J. E. (1999) in *Hematopoiesis*, ed. Zon, L. I. (Oxford Univ. Press, New York), in press.